A NLOS-robust TOA positioning filter based on a skew-t measurement noise model

Henri NURMINEN*, Tohid ARDESHIRI†, Robert PICHÉ*, and Fredrik GUSTAFSSON†

*Department of Automation Science and Engineering, Tampere University of Technology, Finland
{henri.nurminen, robert.piche}@tut.fi
†Division of Automatic Control, Linköping University, Sweden
{tohid, fredrik}@isy.liu.se

Abstract—A skew-t variational Bayes filter (STVBF) is applied to indoor positioning with time-of-arrival (TOA) based distance measurements and pedestrian dead reckoning (PDR). The proposed filter accommodates large positive outliers caused by occasional non-line-of-sight (NLOS) conditions by using a skew-t model of measurement errors. Real-data tests using the fusion of inertial sensors based PDR and ultra-wideband based TOA ranging show that the STVBF clearly outperforms the extended Kalman filter (EKF) in positioning accuracy with the computational complexity about three times that of the EKF.

Keywords—*indoor positioning, TOA, UWB, NLOS, robust filtering, skewness, skew t, variational Bayes*

I. INTRODUCTION

In line-of-sight (LOS) conditions ultra-wideband (UWB) radio's time-of-arrival (TOA) measurements provide ranging accuracy of tens of centimeters. However, non-line-of-sight (NLOS) can reduce the estimation accuracy drastically by introducing a positive measurement bias whose magnitude can be several meters [1]. This is a serious problem in UWB-based indoor positioning because indoor environments typically contain various obstacles that cause NLOS situations whose modeling is challenging.

The conventional extended Kalman filter (EKF) algorithm for TOA positioning gives large location estimation errors in the NLOS condition [1]. Therefore, several works have proposed using NLOS identification and mitigation procedures that attempt to recognize NLOS from the shape of the received UWB pulse [2]–[4]. However, these methods use more than just the TOA information; they process various features of the underlying UWB pulse at an extra computational cost. Furthermore, NLOS identification always has uncertainties due to complexity of the propagation environments. Monitoring the variance of the ranging error within a sliding time window gives information on changes in the LOS condition [5], but these methods are not recursive. The NLOS condition can also be augmented to the filter state and estimated only through the TOA measurements using e.g. particle filters [6]–[9], or

interacting multiple model filters [10], [11]. However, the computational costs of these methods increase rapidly as the number of UWB beacons increases.

The sensitivity of the EKF to large measurement errors is due to the underlying assumption of normally distributed measurement errors. The normal distribution is light-tailed, that is, errors of several sigmas are very improbable. Therefore, when an outlier measurement is encountered, it overwhelms the motion model's state prediction, which causes large estimation errors. One approach for robustifying TOA positioning against NLOS is to assume a heavy-tailed measurement noise distribution [12].

This article proposes applying the recursive skew-t variational Bayes filter (STVBF) [13] to TOA positioning in mixed LOS/NLOS condition fused with inertial measurement based pedestrian dead reckoning (PDR). To our knowledge this is the first work to implement time-series TOA positioning and sensor fusion with PDR using the skew-t model and real-world data. The skew t-distribution is also applied to range-based positioning in [14], but that work considers static estimation with the expectation–maximization algorithm. Neither [13] nor [14] validate the models and methods with real-data tests.

The proposed filter assumes that the measurement noise follows the skew t-distribution, and approximates the posterior distribution using a variational Bayes (VB) approximation [15, Ch. 10]. The skew t-distribution produces occasional large outliers and is skewed, allowing asymmetric distribution of errors around the mean value. Furthermore, the skew t-distribution allows some negative outliers too, thus accounting also for outliers due to e.g. false pulse detections. The STVBF does not require a separate NLOS identification method, but relies only on comparison with the other measurements and the filter prior distribution.

The structure of this paper is the following: First, the skew t-distribution and the STVBF algorithm are explained in detail. Second, it is explained how the STVBF can be used for positioning with UWB and inertial measurements. Finally, the proposed method is tested in indoor environments with real UWB data that are fused with an inertial measurement based motion model. The proposed algorithm is shown to outperform the conventional EKF algorithm at the cost of a moderately increased computational burden.

II. SKEW t-DISTRIBUTION FOR TOA MEASUREMENT

This paper assumes that the TOA measurements from different beacons are independently univariate skew-t-distributed. This definition of the univariate skew t-distribution was originally proposed in multivariate forms by [16]–[18]. The univariate skew t-distribution is parametrized by its location

parameter $\mu \in \mathbb{R}$, spread parameter $\sigma \in \mathbb{R}^+$, shape parameter $\delta \in \mathbb{R}$ and degrees of freedom $\nu \in \mathbb{R}^+$, and has a probability density function (PDF)

$$\mathrm{ST}(z; \mu, \sigma^2, \delta, \nu) = 2\,\mathrm{t}(z; \mu, \delta^2 + \sigma^2, \nu)\,\mathrm{T}(\widetilde{z}; 0, 1, \nu + 1), \tag{1}$$

where

$$\mathrm{t}(z; \mu, \sigma^2, \nu) = \frac{\Gamma\left(\frac{\nu+1}{2}\right)}{\sigma\sqrt{\nu\pi}\Gamma\left(\frac{\nu}{2}\right)}\left(1 + \frac{(z-\mu)^2}{\nu\sigma^2}\right)^{-\frac{\nu+1}{2}} \tag{2}$$

is the PDF of Student's t-distribution, $\Gamma(\cdot)$ is the gamma function, $\widetilde{z}$ is defined by

$$\widetilde{z} \triangleq \frac{(z-\mu)\delta}{\sigma}\left(\frac{\nu+1}{\nu(\delta^2 + \sigma^2) + (z-\mu)^2}\right)^{\frac{1}{2}}, \tag{3}$$

and $\mathrm{T}(\cdot; 0, 1, \nu)$ is the cumulative distribution function (CDF) of Student's t-distribution with degrees of freedom ν and scale 1.

In Fig. 1 the PDF of $\mathrm{ST}(z; 0, 1, \delta, 4)$ is plotted for three values of δ, and in Fig. 2 the PDF of $\mathrm{ST}(z; 0, 1, 1, \nu)$ is plotted for three values of ν. Figures 1 and 2 also show the mean values of the skew t-distributions to demonstrate the fact that the mean is not smaller than than the mode that is again not smaller than the location parameter μ. With $\nu \leq 1$ the mean does not exist. The expressions for the first two moments of the univariate skew t-distribution with the parametrization (1) can be found in [19], [20]. The sign of δ is the sign of skewness, and the skew t-distribution becomes the normal distribution when $\nu \to \infty$ and $\delta \to 0$,

A useful representation of the skew t-distribution is the hierarchical representation [21]

$$z|u, \lambda \sim \mathcal{N}(\mu + \delta u, \lambda^{-1}\sigma^2), \tag{4a}$$
$$u|\lambda \sim \mathcal{N}_+(0, \lambda^{-1}), \tag{4b}$$
$$\lambda \sim \mathcal{G}\left(\frac{\nu}{2}, \frac{\nu}{2}\right), \tag{4c}$$

where u and λ are scalar random variables and $\mathcal{N}_+(m, s^2)$ denotes the truncated normal distribution with closed positive orthant as support, location parameter m, and scale-parameter s. Furthermore, $\mathcal{G}(\alpha, \beta)$ denotes the gamma distribution with shape parameter α and rate parameter β.

The hierarchical representation (4) introduces two latent variables, u and λ. The representation shows that a skew-t-distributed random variable is a sum of a conditionally normal random variable and an independent conditionally truncated-normal random variable where the conditioning is on the gamma-distributed factor λ. Roughly speaking, u being always positive produces the asymmetric deviation, and small λ realisations generate outliers that may be several standard deviations away from the mean, which produces the heavy-tailedness.

III. VARIATIONAL BAYES FOR SKEW-t MEASUREMENT NOISE

The formulas of a filter based on a VB approximation for state-space models with skew-t-distributed measurement noise are presented in [13], and the derivations are given in [22]. The filter computes an approximation of the posterior distribution of x_k for the dynamical model

$$x_{k+1} = A_k x_k + w_k, \qquad w_k \overset{\text{iid}}{\sim} \mathcal{N}(0, Q), \tag{5a}$$
$$y_k = C_k x_k + e_k, \qquad [e_k]_i \overset{\text{iid}}{\sim} \mathrm{ST}(\mu_i, \sigma^2, \delta, \nu) \tag{5b}$$
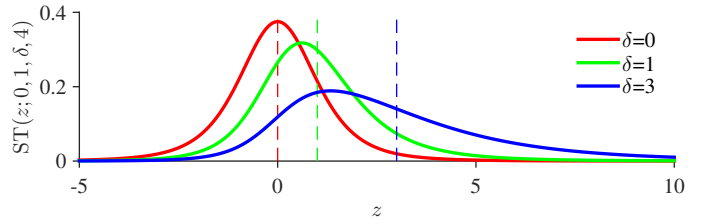

Figure 1. The PDF of $\mathrm{ST}(z; 0, 1, \delta, 4)$ for different values of δ. Dashed lines show the mean values. $\delta = 0$ gives Student's t-distribution, and increasing the absolute value of δ increases skewness.
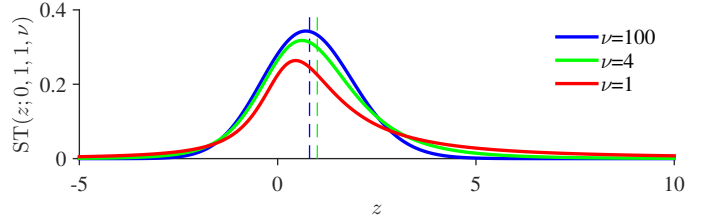

Figure 2. The PDF of $\mathrm{ST}(z; 0, 1, 1, \nu)$ for different values of ν. Dashed lines show the mean values for $\nu > 1$. $\nu = \infty$ gives the skew normal distribution, and decreasing ν increases heavy-tailedness. As for the Student's t-distribution the mean does not exist for $\nu \leq 1$.

where $A_k \in \mathbb{R}^{n_x \times n_x}$ is the state transition matrix; $x_k \in \mathbb{R}^{n_x}$ is the state to be estimated with the prior distribution

$$p(x_1) = \mathcal{N}(x_1; x_{1|0}, P_{1|0}), \tag{6}$$

where the subscript "$a|b$" means "at time a using measurements up to time b" and $\mathcal{N}(\cdot; m, S)$ denotes a (multivariate) normal PDF with mean m and covariance matrix S; $y_k \in \mathbb{R}^{n_y}$ are the measurements, and the elements of the measurement noise vector $e_k \in \mathbb{R}^{n_y}$ are independently skew-t-distributed; $\mu \in \mathbb{R}^{n_y}$ is the vector of location parameters of the measurement noise distribution; $\sigma \in \mathbb{R}^+$ is the spread parameter; $\delta \in \mathbb{R}$ is the shape parameter; $\nu \in \mathbb{R}^+$ is the degrees of freedom; and $C_k \in \mathbb{R}^{n_y \times n_x}$ is the measurement model matrix.

The filtering posterior $p(x_k|y_{1:k})$ is not analytically tractable. However, when the predicted filtering density $p(x_k|y_{1:k-1})$ is normal, the hierarchical representation of the likelihood in (4) enables the VB approximation of the full filtering posterior given by

$$p(x_k, u_k, \Lambda_k|y_{1:k}) \propto p(x_k|y_{1:k-1})p(y_k|x_k, u_k, \Lambda_k) \\ \times p(u_k|\Lambda_k)p(\Lambda_k). \tag{7}$$

In (7), $u_k \in \mathbb{R}^{n_y}$ is a vector and $\Lambda_k \in \mathbb{R}^{n_y \times n_y}$ is a diagonal matrix whose diagonal elements $[\Lambda_k]_{ii}$ have independent gamma-priors of (4c). The VB method [15, Ch. 10] finds the approximation for the joint posterior in the form

$$p(x_k, u_k, \Lambda_k|y_{1:k}) \approx q_x(x_k)q_u(u_k)q_\Lambda(\Lambda_k) \tag{8}$$

from which an approximation of the marginal $p(x_k|y_{1:k})$ can be obtained. The approximate distributions $q_x(x_k)$, $q_u(u_k)$ and $q_\Lambda(\Lambda_k)$ are chosen such that they minimize the Kullback-Leibler divergence (KLD) [23] of the true posterior from the factorized approximation on the right hand side of (8):

$$\hat{q}_x, \hat{q}_u, \hat{q}_\Lambda = \underset{q_x, q_u, q_\Lambda}{\mathrm{argmin}} \\ D_{\mathrm{KL}}(q_x(x_k)q_u(u_k)q_\Lambda(\Lambda_k)||p(x_k, u_k, \Lambda_k|y_{1:k})) \tag{9}$$

where $D_{\mathrm{KL}}(q(\cdot)||p(\cdot)) \triangleq \int q(x)\log\frac{q(x)}{p(x)}\,\mathrm{d}x$ is the KLD. The VB method results in an iterative algorithm presented in

Table I.   SKEW-t VARIATIONAL BAYES FILTER

1: **Inputs:** A_k, C_k, Q, μ, σ^2, δ, ν, $x_{1|0}$, $P_{1|0}$, $y_{1:K}$ and N_{VB}
2: **for** $k = 1$ to K **do**
    initialization
3:    $\Lambda_k \leftarrow I_{n_y \times n_y}$
4:    $\overline{u_k} \leftarrow 0_{n_y \times 1}$
5:    $\Upsilon \leftarrow 0_{n_y \times n_y}$
6:    $K_u \leftarrow \delta(\delta^2 + \sigma^2)^{-1} \cdot I_{n_y \times n_y}$
7:    **for** $j = 1$ to N_{VB} **do**
        update $q_x(x_k) = \mathcal{N}(x_k; x_{k|k}, P_{k|k})$ given $q_u(u_k)$ and $q_\Lambda(\Lambda_k)$
8:        $K_x \leftarrow P_{k|k-1} C_k^{\mathrm{T}} (C_k P_{k|k-1} C_k^{\mathrm{T}} + \sigma^2 \overline{\Lambda_k}^{-1})^{-1}$
9:        $x_{k|k} \leftarrow x_{k|k-1} + K_x(y_k - \mu - C_k x_{k|k-1} - \delta\overline{u_k})$
10:       $P_{k|k} \leftarrow (I - K_x C_k)P_{k|k-1}$
        update $q_u(u_k) = \mathcal{N}_+(u_k; u_{k|k}, U_{k|k})$ given $q_x(x_k)$ and $q_\Lambda(\Lambda_k)$
11:       $\widetilde{u}_k \leftarrow y_k - \mu - C_k x_{k|k}$
12:       $u_{k|k} \leftarrow K_u \widetilde{u}_k$
13:       $U_{k|k} \leftarrow (I - \delta K_u)\overline{\Lambda_k}^{-1}$
14:       **for** $i = 1$ to n_y **do**
15:          $\xi \leftarrow \frac{[u_{k|k}]_i}{[U_{k|k}]_{ii}}$
16:          $\epsilon \leftarrow \frac{\phi(\xi)}{\Phi(\xi)}$, ϕ is the PDF and Φ the CDF of $\mathcal{N}(0,1)$
17:          If $\Phi(\xi)$ underflows to zero, set $[\overline{u_k}]_i \leftarrow 0$ and $\Upsilon_{ii} \leftarrow 0$
18:          $[\overline{u_k}]_i \leftarrow [u_{k|k}]_i + \epsilon\sqrt{[U_{k|k}]_{ii}}$
19:          $\Upsilon_{ii} \leftarrow [U_{k|k}]_{ii} \cdot (1 - \xi\epsilon - \epsilon^2) + [\overline{u_k}]_i^2$
20:       **end for**
        update $q_\Lambda(\Lambda_k) = \prod_{i=1}^{n_y} \mathcal{G}\left([\Lambda_k]_{ii}; \frac{\nu}{2} + 1, \frac{\nu + [\Psi_k]_{ii}}{2}\right)$
        given $q_u(u_k)$ and $q_x(x_k)$
21:       $\Psi \leftarrow \frac{1}{\sigma^2}(\widetilde{u}_k \widetilde{u}_k^{\mathrm{T}} + C_k P_{k|k} C_k^{\mathrm{T}}) + (\frac{\delta^2}{\sigma^2} + 1)\Upsilon$
             $- \frac{\delta^2}{\sigma^2}(\overline{u_k}\widetilde{u}_k^{\mathrm{T}} + \widetilde{u}_k \overline{u_k}^{\mathrm{T}})$
22:       $[\overline{\Lambda_k}]_{ii} \leftarrow \frac{\nu+2}{\nu+\Psi_{ii}}$
23:    **end for**
    predict $q_x(x_{k+1})$
24:    $x_{k+1|k} \leftarrow A_k x_{k|k}$
25:    $P_{k+1|k} \leftarrow A_k P_{k|k} A_k^{\mathrm{T}} + Q$
26: **end for**
27: **Outputs:** $x_{k|k}$ and $P_{k|k}$ for $k = 1 \cdots K$

Table I. With the skew-t measurement noise the approximative marginal posterior of x_k is a normal distribution with the parametrization $q_x(x_k) = \mathcal{N}(x_k; x_{k|k}, P_{k|k})$, where the parameters $x_{k|k}$ and $P_{k|k}$ are the output of the STVBF algorithm of Table I. Because the algorithm uses a normal prior and results in a normal posterior approximation, it provides a Kalman filter -type recursive solution to the inference problem outlined in (5).

IV. FUSION OF UWB RANGING AND PDR

This section explains how the measurements of UWB ranging and inertial measurement based PDR can be used in the general filtering framework of Table I to produce a fused estimate for the user's position. Inertial measurement based PDR produces a continuous and relatively accurate estimate of the change in the user's position. However, due to the need of initial position estimate and the sensor drift it has to be complemented by some absolute position information such as UWB. Correspondingly, the UWB ranging has high absolute accuracy, but the precise motion model provided by the PDR helps in detecting NLOS outliers.

A. Motion model from PDR

The proposed positioning system uses a PDR solution based on inertial sensors, i.e. three-axis accelerometers and gyroscopes. The used PDR solution's output is footstep detection and measurements of the horizontal-plane heading change ψ_k.

The footsteps are detected using the accelerometer output's norm [24]. The accelerometers also show the direction of gravity which gives the horizontal plane, and the user's heading change during a footstep is then estimated from the gyroscope's angular velocity measurements projected to the horizontal plane [25].

The sensor fusion algorithm uses a linear motion model based on this PDR solution. The method is proposed for 2-dimensional positioning in [26], and in this paper the altitude of the user equipment is also in the state. The state vector is $x_k = \begin{bmatrix} l_k \\ s_k \end{bmatrix}$, where $l_k \in \mathbb{R}^3$ is the user equipment's 3-dimensional position and $s_k \in \mathbb{R}^2$ is the horizontal footstep vector. At a time update, the step vector is rotated by the heading change ψ_k and affected by process noise, and the x and y coordinates are updated by the step vector. The altitude process is modeled as a random walk. The state transition matrix and the process noise covariance matrix in (5a) are thus

$$A_k = \begin{bmatrix} 1 & 0 & 0 & 1 & 0 \\ 0 & 1 & 0 & 0 & 1 \\ 0 & 0 & 1 & 0 & 0 \\ 0 & 0 & 0 & \cos\overline{\psi_k} & -\sin\overline{\psi_k} \\ 0 & 0 & 0 & \sin\overline{\psi_k} & \cos\overline{\psi_k} \end{bmatrix}, \quad (10)$$

$$Q = \text{Diag}(0, 0, \sigma_h^2, \sigma_s^2, \sigma_s^2), \quad (11)$$

respectively [26]. Here $\overline{\psi_k}$ is the heading change estimate given by the PDR solution, σ_s^2 is a variance parameter that models the uncertainty of the PDR measurements and the step length's process noise, and σ_h^2 is the altitude's process noise variance. Because this motion model is linear, it is free from linearization errors that occur when the velocity is unknown, but the model cannot model the uncertainties of the PDR as flexibly as some conventional non-linear models [26].

If PDR is not used, positioning can be done with UWB alone by adopting a less informative motion model. This can be a white noise based kinematic model [27, Ch. 6], for example.

B. Measurement model from UWB ranging

A TOA measurement gives the distance traveled by the radio wave between the UWB beacon and the user. To account for occasional large positive measurement errors due to non-line-of-sight conditions, the measurement noise of all sensors is assumed to be identically and independently skew-t-distributed:

$$[y_k]_i = \|l_k - b_i\| + [e_k]_i, \ [e_k]_i \overset{\text{iid}}{\sim} \text{ST}(\mu, \sigma^2, \delta, \nu), \quad (12)$$

where $y_k \in \mathbb{R}^{n_y}$ is the TOA-based distance vector, l_k is the user position, $b_i \in \mathbb{R}^3$ is the 3-dimensional position of the ith UWB beacon, and e_k is measurement noise.

The model (5) and the STVBF assume a linear measurement model, while (12) is nonlinear. This limitation can be overcome by linearizing the model at the prior mean $x_{k|k-1} = \begin{bmatrix} l_{k|k-1} \\ s_{k|k-1} \end{bmatrix}$, giving

$$y_k = C_k x_k + e_k, \quad (13)$$

where the ith row of C_k is

$$[C_k]_i = \begin{bmatrix} \frac{(l_{k|k-1}-b_i)^{\mathrm{T}}}{\|l_{k|k-1}-b_i\|} & \text{O}_{1\times 2} \end{bmatrix}, \quad (14)$$

and

$$[e_k]_i \sim \text{ST}\left(\mu + \|l_{k|k-1} - b_i\| - [C_k]_i x_{k|k-1}, \sigma^2, \delta, \nu\right). \quad (15)$$

Hence, the approximative measurement equations (13) and (15) are in the form of (5b).
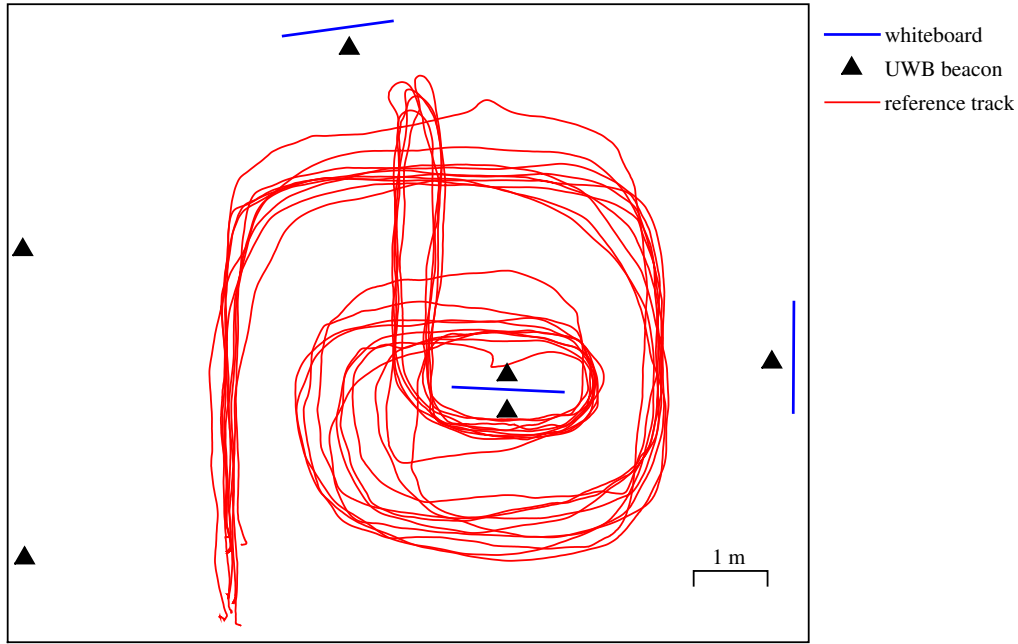
Figure 4.   Layout of the testing area. NLOS condition is created by the whiteboard at the center of the testing area.

Figure 3.   A SpoonPhone and a BeSpoon UWB tag.

V.   REAL-DATA TESTS

Real UWB measurements were collected to evaluate the proposed method's performance. The measurement equipment was a Spoonphone smartphone [28] with Android 4.2 operating system and UWB channel 2 pulse radio (3993.6 MHz, 500 MHz bandwidth), and six BeSpoon UWB tags. Fig. 3 shows a picture of the equipment. The system uses two-way TOA ranging, and so it does not depend on clock synchronization. The used inertial sensors were the Spoonphone's built-in sensors. The UWB measurement update was done with 2 Hz frequency, and the error computation for obtaining the error statistics was also done with 2 Hz frequency. Five test tracks were collected in a laboratory environment and three test tracks in a real indoor environment of a university campus. The algorithms were computed with MATLAB.

The estimation algorithm for the skew-t noise is the STVBF in Table I. The parameters of the skew-t noise distribution, $\{\mu, \sigma^2, \delta, \nu\}$, were optimized to minimize the average root-mean-square error (RMSE) of the 2-dimensional positioning error for all the test tracks. The parameter optimization was done using 30 VB iterations (N_{VB}=30), which should ensure

convergence [13]. The optimized parameter values are in Table II. The same data were used for both parameter calibration and positioning tests to obtain a fair comparison of the optimal set-ups of each filtering algorithm. This eliminates the effect of possible differences in calibration and positioning data.

The used motion model parameter values for 2 Hz updating frequency are $\sigma_h = 5 \cdot 10^{-4}$ m and $\sigma_s = 3 \cdot 10^{-2}$ m. Due to the small value of σ_h floor changes need a separate model, but this is out of the scope of this paper.

The STVBF is compared with the EKF that is based on the normal measurement noise model

$$[y_k]_i = \|l_k - b_i\| + e_k, \quad [e_k]_i \overset{\text{iid}}{\sim} \mathcal{N}(\tau, \rho^2). \quad (16)$$

The noise parameters τ and ρ^2 were also optimized for the test track set, and the optimized parameter values are in Table II.

Fig. 5 shows the average RMSE of the STVBF as a function of the number of VB iterations, and its comparison with the EKF's RMSE. Note that the methods use different noise parameter values according to Table II. The figure shows that 2 VB iterations already outperforms the best possible EKF estimate, and 4 VB iterations is enough to achieve the converged state's average RMSE in this scenario.

Table II.   THE USED PARAMETER VALUES OBTAINED BY OPTIMIZING WITH RESPECT TO THE TEST TRACKS' AVERAGE RMSE

Filter	STVBF				EKF	
Param.	μ (m)	σ (m)	δ (m)	ν	τ (m)	ρ (m)
Value	-0.1	0.3	0.6	4	1.3	1.6

Table III.   THE ERROR STATISTICS IN THE LABORATORY ENVIRONMENT WITH OPTIMIZED NOISE PARAMETERS

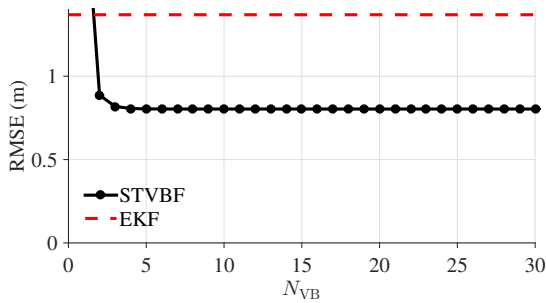| Filter	RMSE (m)	mean (m)	median (m)	95 % quant. (m)	95 % cons. (%)	running time
EKF	1.36	1.16	1.02	2.58	94	1
STVBF	0.56	0.46	0.38	1.16	91	3

Figure 5. STVBF's average RMSE for all the test tracks as a function of the number of VB iterations compared with the EKF's average RMSE. 4 VB iterations is enough for the STVBF in the PDR & UWB-TOA positioning.
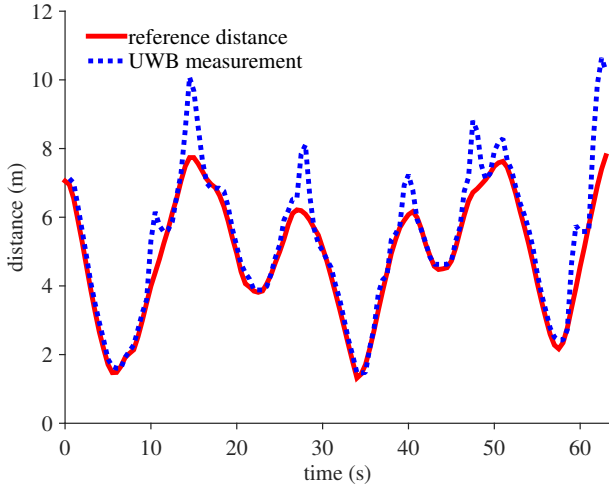

Figure 6. Distance measurement of one laboratory track for one UWB beacon compared with the true distance.

A. Laboratory measurements with high-accuracy reference

One data set was measured in a laboratory environment to obtain high-accuracy reference position[1]. To acquire a realistic simulation of an office-like indoor environment, a whiteboard was placed in the middle of the testing area, and lab personnel moved about in the area to simulate passersby. These obstacles caused occasional NLOS conditions for some UWB beacons. Fig. 4 depicts the testing area and the used test tracks. Fig. 6 compares the distance measurements of one track for one UWB beacon with the reference distance given by the laboratory equipment, and shows that occasional NLOS measurements are visible as positive peaks in the measurement error. Fig. 7 shows that the histogram distribution of these errors is positively skewed.

The error statistics of the STVBF with 4 VB iterations and the EKF are in Table III. The shown accuracy measures are the average RMSE of the five tracks, mean error, median error, empirical 95 % quantile of errors, 95 % consistency, and relative running time averaged over the five test tracks. Consistency is the percentage of time instants when the filter was consistent with respect to the Gaussian NEES (normalized estimation error squared) consistency test [27, Ch. 5.4.2]; the closer the consistency is to 95 %, the more accurately the filter

---

[1]High accuracy reference measurements are provided through the use of the Vicon real-time tracking system courtesy of the UAS Technologies Lab, Artificial Intelligence and Integrated Computer Systems Division (AIICS) at the Department of Computer and Information Science (IDA). http://www.ida.liu.se/divisions/aiics/aiicssite/index.en.shtml
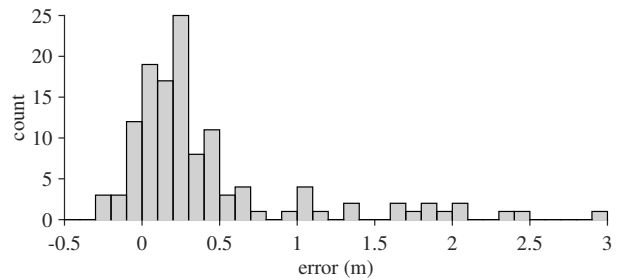

Figure 7. Error histogram of the measurements depicted by Fig. 6.

Table IV. THE ERROR STATISTICS IN THE CAMPUS ENVIRONMENT WITH OPTIMIZED NOISE PARAMETERS

Track	Filter	RMSE (m)	mean (m)	median (m)	95 % quant. (m)	95 % cons. (%)
1	EKF	1.91	1.57	1.20	4.02	83
	STVBF	1.23	1.11	1.04	1.94	41
2	EKF	1.41	1.24	1.21	2.79	95
	STVBF	0.81	0.70	0.63	1.45	59
3	EKF	0.83	0.72	0.67	1.43	98
	STVBF	0.74	0.68	0.73	1.07	55

reports the estimate's uncertainty. The results show that both the filters are fairly consistent, but the STVBF has significantly better accuracy; the STVBF's errors are less than 50 % of the EKF's errors. The computational burden of our STVBF implementation is only three times that of the EKF's, which we consider reasonable for the improvement in performance.

B. Measurements in campus environment

Three test tracks were measured in real indoor environment in a campus building of Tampere University of Technology to ensure that the conclusions based on the laboratory measurements also hold in realistic indoor environment. In these tests the reference position of the user was obtained by matching certain reference points of the track with an indoor map and interpolating the positions between these reference points. Five UWB beacons were used, and the beacon positions were also obtained by matching with a map. These reference positions are not as accurate as those in section V-A, but the accuracy is in the order of tens of centimeters, which is more accurate than the expected positioning accuracy. The maps of the test areas are shown in Figures 8, 9, and 10 for tracks 1, 2, and 3, respectively.

The beacon positions at the tracks 1 and 2 were chosen such that NLOS conditions occur every now and then. Track 1 consists of walking in corridors and turning at two corridor junctions. Track 2 consists of walking in a corridor and visiting an office room. Track 3 contains only walking in a straight corridor, and the time under NLOS condition was minimized in this track to evaluate the algorithms' performance also in pure LOS condition.

The error statistics of the positioning tests in the campus environment are shown in Table IV. In tracks 1 and 2 the STVBF clearly outperforms the EKF in positioning accuracy. In track 3 the performances of the STVBF and EKF are much closer, which is expectable because track 3 mainly contains LOS measurements. However, the STVBF is still slightly more accurate that the EKF in track 3, which might partly be explained by occasional NLOS caused by the body of the person conducting the experiments. The test results indicate that the STVBF outperforms the EKF in mixed LOS/NLOS condition, and performs equally well or better in LOS condition.
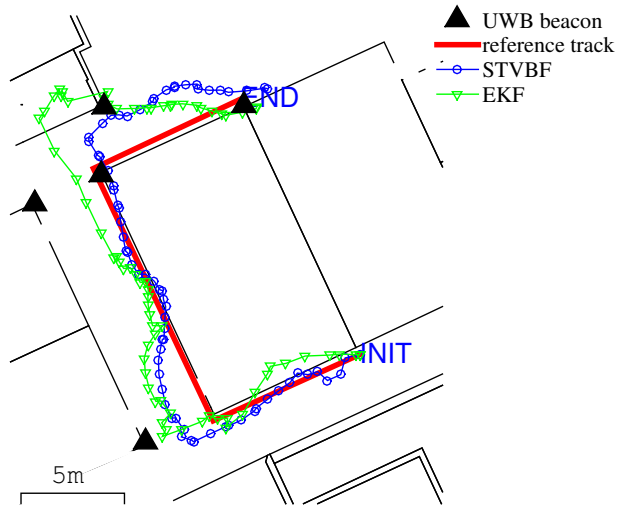
Figure 8. Campus test track 1 consists of corridors and turns at corridor junctions.
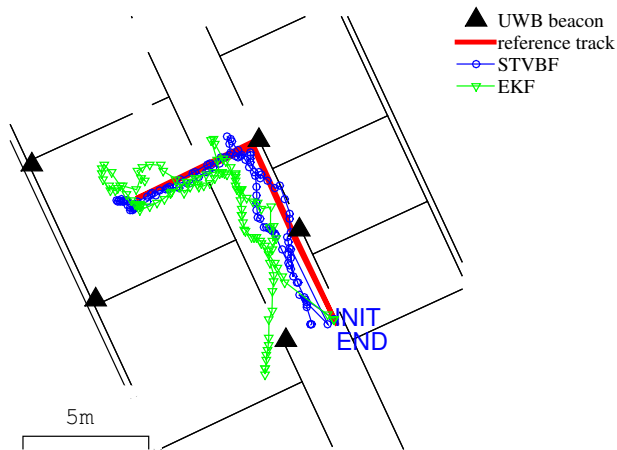

Figure 9. Campus test track 2 consists of a visit in an office room.

Figure 10. In campus test track 3 the tags are in LOS condition most of the time.

VI. Conclusions

The use of the skew-t variational Bayes filter (STVBF) in indoor positioning with inertial sensors and UWB ranging in mixed LOS/NLOS conditions is proposed. The proposed filter is more robust against outliers than the conventional EKF that is based on assumed normality of the measurement noise. Due to the assumption of positively skewed measurement noise, the proposed algorithm is also capable of accounting for the fact that the NLOS phenomena typically cause positive outlier measurements more frequently than negative ones. Real-data tests showed that STVBF enables dramatic improvement in positioning accuracy compared to the EKF with the computational burden of about three EKFs.

References

[1] S. Gezici, Z. Tian, G. B. Giannakis, H. Kobayashi, A. F. Molisch, H. V. Poor, and Z. Sahinoglu, "Localization via ultra-wideband radios: a look at positioning aspects for future sensor networks," *IEEE Signal Processing Magazine*, vol. 22, no. 4, pp. 70–84, July 2005.

[2] I. Güvenç, C.-C. Chong, F. Watanabe, and H. Inamura, "NLOS identification and weighted least-squares localization for UWB systems using multipath channel statistics," *EURASIP Journal on Advances in Signal Processing*, vol. 2008, January 2008.

[3] J. Khodjaev, Y. Park, and A. S. Malik, "Survey of NLOS identification and error mitigation problems in UWB-based positioning algorithms for dense environments," *Annals of Telecommunications*, vol. 65, no. 5–6, pp. 301–311, June 2010.

[4] S. Marano, W. M. Gifford, H. Wymeersch, and M. Z. Win, "NLOS identification and mitigation for localization based on UWB experimental data," *IEEE Journal on Selected Areas in Communications*, vol. 28, no. 7, pp. 1026–1035, September 2010.

[5] C.-D. Wann and C.-S. Hsueh, "NLOS mitigation with biased Kalman filters for range estimation in UWB systems," in *TENCON 2007 - 2007 IEEE Region 10 Conference*, October 2007, pp. 1–4.

[6] B. Denis, L. Ouvry, B. Uguen, and F. Tchoffo-Talom, "Advanced Bayesian filtering techniques for UWB tracking systems in indoor environments," in *2005 IEEE International Conference on Ultra-Wideband (ICU 2005)*, September 2005, pp. 638–643.

[7] J. González, J. Blanco, C. Galindo, A. Ortiz-de Galisteo, J. Fernández-Madrigal, F. Moreno, and J. Martínez, "Mobile robot localization based on ultra-wide-band ranging: A particle filter approach," *Robotics and Autonomous Systems*, vol. 57, no. 5, pp. 496–507, May 2009.

[8] L. Chen, R. Piché, H. Kuusniemi, and R. Chen, "Adaptive mobile tracking in unknown non-line-of-sight conditions with application to digital TV networks," *EURASIP Journal on Advances in Signal Processing*, vol. 22, no. 1, p. 10 pp., February 2014.

[9] E. Özkan, F. Lindsten, C. Fritsche, and F. Gustafsson, "Recursive maximum likelihood identification of jump Markov nonlinear systems," *IEEE Transactions on Signal Processing*, vol. 63, no. 3, pp. 754–765, February 2015.

[10] J.-F. Liao and B.-S. Chen, "Robust mobile location estimator with NLOS mitigation using Interacting Multiple Model algorithm," *IEEE Transactions on Wireless Communications*, vol. 5, no. 11, pp. 3002–3006, November 2006.

[11] C. Fritsche, U. Hammes, A. Klein, and A. M. Zoubir, "Robust mobile terminal tracking in NLOS environments using interacting multiple model algorithm," in *2009 IEEE International Conference on Acoustics, Speech and Signal Processing (ICASSP 2009)*, April 2009, pp. 3049–3052.

[12] F. Gustafsson and F. Gunnarsson, "Mobile positioning using wireless networks: possibilities and fundamental limitations based on available wireless network measurements," *IEEE Signal Processing Magazine*, vol. 22, no. 4, pp. 41–53, July 2005.

[13] H. Nurminen, T. Ardeshiri, R. Piché, and F. Gustafsson, "Robust inference for state-space models with skewed measurement noise," *IEEE Signal Processing Letters*, vol. 22, no. 11, pp. 1898–1902, November 2015.

[14] P. Müller and R. Piché, "Statistical trilateration with skew-t errors," in *International Conference on Localization and GNSS (ICL-GNSS 2015)*, June 2015.

[15] C. M. Bishop, *Pattern Recognition and Machine Learning*. Springer, 2007.
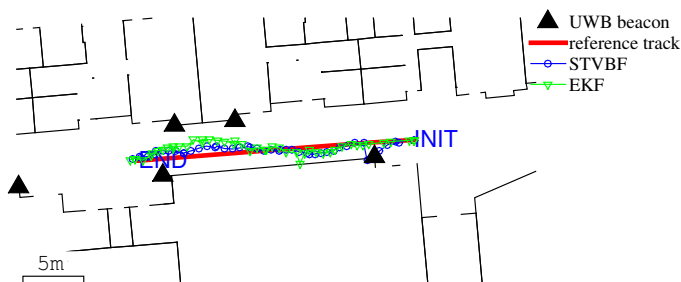
[16] M. D. Branco and D. K. Dey, "A general class of multivariate skew-elliptical distributions," *Journal of Multivariate Analysis*, vol. 79, no. 1, pp. 99–113, October 2001.

[17] A. Azzalini and A. Capitanio, "Distributions generated by perturbation of symmetry with emphasis on a multivariate skew t-distribution," *Journal of the Royal Statistical Society. Series B (Statistical Methodology)*, vol. 65, no. 2, pp. 367–389, 2003.

[18] A. K. Gupta, "Multivariate skew t-distribution," *Statistics*, vol. 37, no. 4, pp. 359–363, 2003.

[19] S. K. Sahu, D. K. Dey, and M. D. Branco, "A new class of multivariate skew distributions with applications to Bayesian regression models," *Canadian Journal of Statistics*, vol. 31, no. 2, pp. 129–150, 2003.

[20] ——, "Erratum: A new class of multivariate skew distributions with applications to Bayesian regression models," *Canadian Journal of Statistics*, vol. 37, no. 2, pp. 301–302, 2009.

[21] T.-I. Lin, "Robust mixture modeling using multivariate skew t distributions," *Statistics and Computing*, vol. 20, pp. 343–356, 2010.

[22] T. Ardeshiri, H. Nurminen, R. Piché, and F. Gustafsson, "Variational iterations for filtering and smoothing with skew-t measurement noise," Department of Electrical Engineering, Linköping University, SE-581 83 Linköping, Sweden, Tech. Rep. LiTH-ISY-R-3076, March 2015. [Online]. Available: http://urn.kb.se/resolve?urn=urn:nbn:se:liu:diva-115741

[23] T. M. Cover and J. Thomas, *Elements of Information Theory*. John Wiley and Sons, 2006.

[24] H. Leppäkoski, J. Collin, and J. Takala, "Pedestrian navigation based on inertial sensors, indoor map, and WLAN signals," *Journal of Signal Processing Systems*, vol. 71, no. 3, pp. 287–296, June 2013.

[25] J. Collin, O. Mezentsev, and G. Lachapelle, "Indoor positioning system using accelerometry and high accuracy heading sensors," in *GPS/GNSS 2003 Conference (Session C3)*, Portland, OR, September 2003.

[26] M. Raitoharju, H. Nurminen, and R. Piché, "Kalman filter with a linear state model for PDR+WLAN positioning and its application to assisting a particle filter," *EURASIP Journal on Advances in Signal Processing*, no. 33, April 2015.

[27] Y. Bar-Shalom, R. X. Li, and T. Kirubarajan, *Estimation with Applications to Tracking and Navigation, Theory Algorithms and Software*. John Wiley & Sons, 2001.

[28] The SpoonPhone. [Online]. Available: http://spoonphone.com/en/